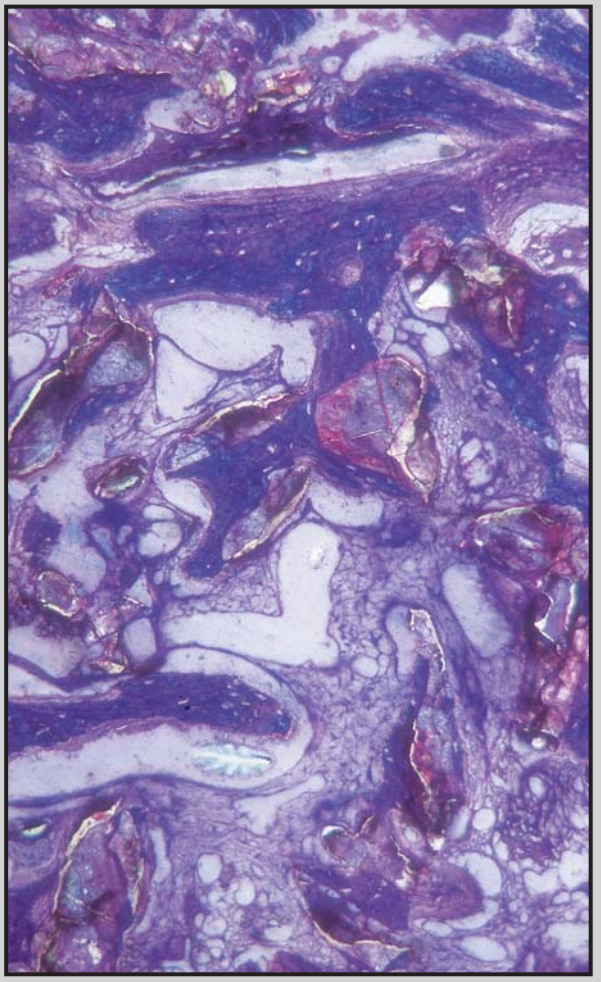

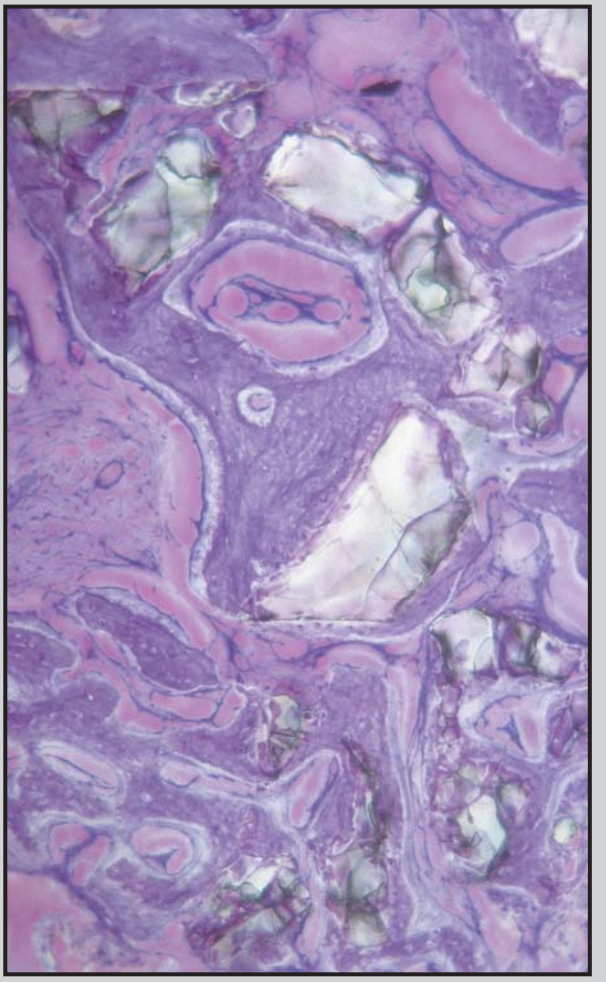

Sinus Graft with Biogran, Autogenous Bone, and PRP: A Report of Three Cases with Histology and Micro-CT

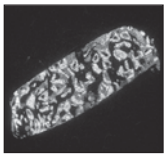

*Paolo Trisi, MD, DDS, PhD**
*Alberto Rebaudi, MD, DDS***
*Federica Calvari, DDS****
*Richard J. Lazzara, DMD, MScD*****

Three sinuses were grafted with a bioactive glass bone substitute (Biogran) mixed with autogenous bone retrieved from intraoral donor sites. In two of the three sinuses a platelet-rich plasma (PRP) gel was added to the graft. Bone biopsies retrieved after 5, 6, and 15 months were analyzed. Micro–computerized tomography (micro-CT) values of total bone volume/total volume (TBV/TV) were very reliable compared to histomorphometry. Biogran mixed with autogenous bone and PRP seems to have a positive effect in sinus grafting, with TBV/TV values ranging between 40% and 68%. Micro-CT results have never been compared with histomorphometry for the evaluation of grafted biomaterials. Micro-CT evaluation of some morphometric parameters was difficult, because the radiodensities of Biogran and a certain grade of bone mineralization were similar. (Int J Periodontics Restorative Dent 2006;26:113–125.)

*Private Practice, Pescara, Italy; Scientific Director, Biomaterials Clinical Research Association, Pescara, Italy.
**Private Practice, Genova, Italy; Secretary, Biomaterials Clinical Research Association, Pescara, Italy.
***Private Practice, Genova, Italy.
****Private Practice, West Palm Beach, Florida.

Correspondence to: Dr Paolo Trisi, Via San Silvestro 163/3, 65132 Pescara, Italy; fax: +390-85-693351; e-mail: paulbioc@tin.it.

The edentulous posterior maxilla often presents with insufficient bone quality and quantity to achieve predictable rehabilitation with endosseous oral implants.[1–3] Crestal bone resorption and pneumatization of the maxillary sinus are often evident after loss of posterior teeth.[4,5]

Clinical success has been obtained by grafting the maxillary sinus with different materials,[2,6,7] including autogenous bone, either in blocks from extraoral donor sites[8] or minced into particles.[2,9] Sinus grafting procedures have been proposed before or simultaneously with implant placement.[2,9–11] New bone formation after sinus graft procedures has been demonstrated by the use of histologic analysis in animals[12] and in humans.[13–15]

A consensus conference on the subject of sinus floor elevation in 1996[4] summarized the bases of the clinical experience of 38 surgeons, who had placed 3,554 implants in 1,007 posterior maxillae using bone and various bone substitutes and a combination of different grafting materials. Because the data from the consensus conference[4] were so multivariate and multifactorial, definite conclusions could not

be drawn, and clinicians await controlled prospective studies to better understand which are the best materials and techniques.

Dental research employs qualitative and quantitative morphometry as methods to evaluate bone integration of dental implants, biomaterials, and regenerative procedures.[16,17] Bone histomorphometry[18–21] allows the evaluation of many parameters, such as bone volume (bone volume/total volume, or BV/TV) and bone structure, including trabecular thickness, trabecular separation, and trabecular number. Dynamic parameters (eg, bone formation and resorption rate, bone balance) can also be evaluated by labeling bone with tetracyclines. These parameters are able to give many indications about the development of bone tissue during the healing period or when subjected to a functional load.[18–23]

Bone morphometric analysis has traditionally been assessed in two-dimensional (2D) histologic sections, with a third dimension added on the basis of stereology. In an attempt to better evaluate bone connectivity, other three-dimensional (3D) procedures have been proposed.[24,25] Micro–computerized tomography (micro-CT) scanning is a nondestructive alternative approach to outline and quantify bone in three dimensions, allowing higher-resolution 3D images and quantitative measurements of the trabecular bone structure.[26,27]

The histologic processing of bone biopsies containing alloplastic implants is a destructive procedure,[28] and the measurement technique for bone histomorphometric analysis is tedious and time consuming.[29] However, the histologic process allows high resolution, good image contrast, and a large number of evaluations, including that of number and type of cells.[30]

The development of regenerated bone tissues has not been fully clarified from a biomechanical viewpoint, especially when biomaterials are used as bone substitutes. It is therefore important to analyze 3D bone architecture and its relationship to the biomaterials used to better clarify the biomechanical implications of regenerated bone, since bone regeneration is often performed to obtain a functional strong anchorage for implants. Because bone substitutes are often used for sinus grafts, the need for more studies is evident, especially for such characteristics as the ability to conduct bone, the ability to be resorbed after healing, and their functional behavior when bone is subjected to different load conditions.

The aim of the present study was to evaluate bone biopsies from the grafted sinuses of three patients. Biopsies from the patients were evaluated with standard histomorphometry and micro-CT. The values obtained with the two different techniques were compared to verify the reliability of the micro-CT technique as a new way to the evaluate bone samples containing hard biomaterials.

Method and materials

Three patients in good general health who required dental implants in the posterior atrophic maxilla gave written informed consent. Each received a bone graft in the maxillary sinus composed of a ceramic bone substitute (Biogran, 3i Implant Innovations) mixed with autogenous bone chips retrieved from intraoral donor sites, with the addition of an autogenous gel of platelet-rich plasma (PRP) in two of the three cases. Biogran was used to augment the autogenous bone. The volume needed was determined by required implant length. PRP gel was added because autogenous bone was part of the graft, and PRP should positively affect the cellular component of the autogenous bone graft.

After 20, 24, and 60 weeks of healing, during the surgical re-entry for implant placement, a bone biopsy was retrieved from each sinus and fixed for morphometric analysis. After removal, the specimens were sent to the laboratory of the Biomaterials Clinical Research Association, Pescara, Italy, and processed for micro-CT and histologic examination. Initially, the samples were embedded in resin and analyzed by 3D micro-CT (Scanco Medical); subsequently, histologic sections were prepared for standard histomorphometric measurements.

Sample preparation

Bone biopsies were immediately rinsed in saline, fixed in 10% formalin, and processed to obtain thin ground sections. The specimens were dehydrated in an ascending series of alcohol rinses and then embedded in acrylic resin. After polymerization, the specimens were ready for micro-CT examination.

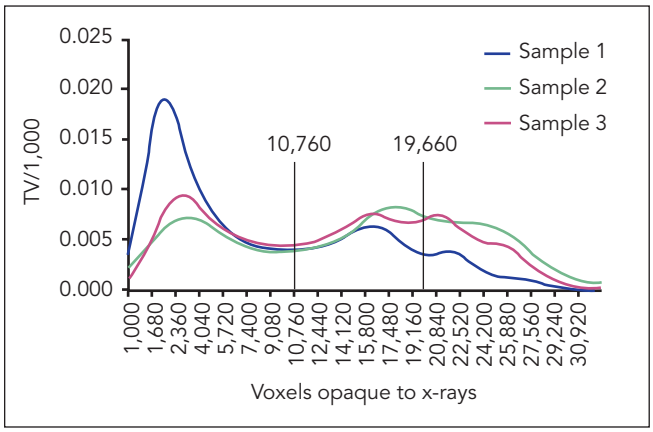

Fig 1 *Histogram of grayscale values normed to TV. The gray-level distribution allows distinction of the different materials. Peaks under the threshold of 10,760 indicate soft tissues, peaks between 10,760 and 19,660 indicate bone, and peaks over 19,660 indicate the radiopaque particles of the grafting materials (autogenous bone particles and Biogran).*

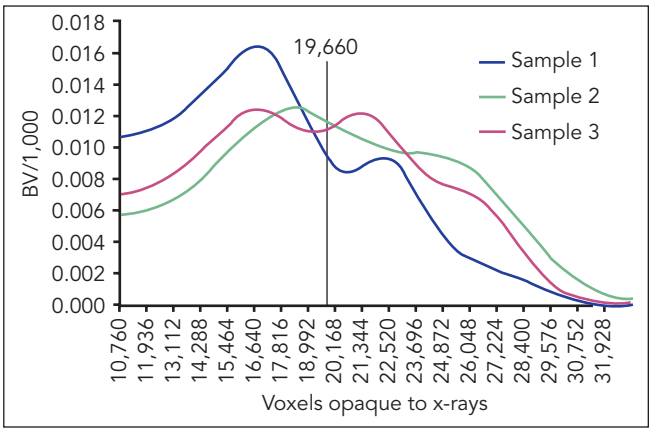

Fig 2 *Histogram of grayscale values normed to BV. Peaks under the threshold of 19,660 indicate bone and peaks over 19,660 indicate Biogran. From this graphic it is evident that the radiodensity of Biogran and that of a certain grade of bone mineralization are very similar.*

Micro-CT processing

The specimens were scanned with a high-resolution micro-CT system (μ-CT-20, Scanco Medical) in multislice mode. Each 3D image data set consisted of approximately 400 micro-CT slice images (1,024 × 1,024 pixels with 16-bit grey levels).[27,31]

The specimens were scanned in high-resolution mode with an x, y, and z resolution of about 20 μm. The voxel size was 15 × 15 × 15 μm^3. Scanning time for each specimen was approximately 4 hours. Micro-CT measurement of the bone/graft was obtained by working on the thresholds of the gray levels. After scanning, the 3D data sets were segmented by using two different thresholds for bone and the ceramic biomaterial to separate the different materials. The first threshold was set to 10,760 (arbitrary units that correspond to density) to view both the bone and the graft; the second threshold was set at 19,660 (arbitrary units that correspond to density) to view the graft only. The threshold values were determined by analyzing the gray-level distribution (histogram analysis) and picking up the intermediate gray-level value between the two peaks of the materials to be distinguished (Figs 1 and 2).

With the arbitrary threshold of 19,660, it was possible to visualize and measure only the graft (autogenous bone chips and Biogran granules), since this threshold hides new bone tissue, which is generally lower in density, thus allowing measurement of graft particles only (see Fig 2). By subtracting the measurement of graft volume (GV/TV) from the measurement of all bone + graft volume (total bone volume [TBV] /TV), the measurement of bone volume (BV/TV) was determined.

Histologic processing

After the micro-CT scanning of the samples was completed, the specimens were sectioned at 200 to 250 μm by a Micromet high-speed rotating blade microtome and subsequently ground down to about 40 to 50 μm by an LS2 grinding machine (Remet). The histologic slides were routinely stained with toluidine blue and basic fuchsin. Three sections were produced for each biopsy.

The histomorphometric analysis was performed by digitizing the images from the microscope via a JVC TK-C1380 Color Video Camera (JVC Victor Company) and a frame grabber. Subsequently, the digitized images were analyzed by the image analysis software IAS 2000 (Delta Sistemi). The images were acquired with a 5× objective all around the implant surface.

Table 1 Morphometric measurements under micro-CT (μCT) and under conventional histomorphometry (Histo)

	Healing time (mo)	PRP in graft?	TBV/TV (%)		BV/TV (%)		GV/TV (%)		BGC/TGS (%)
			μCT	Histo	μCT	Histo	μCT	Histo	Histo
Sample 1	5	Yes	40	42.52	29	37.53	11	4.99	25.79
Sample 2	15	No	68	65.70	34	49.71	34	15.99	60.17
Sample 3	6	Yes	64	58.85	36	41.32	28	17.53	45.24
Mean	—	—	57.33	55.69	33	42.85	24.33	12.84	43.73
SD	—	—	15.14	12.92	3.60	6.23	11.93	6.84	17.24

TBV/TV = total volume; BV/TV = vital bone volume; GV/TV = graft volume; BGC/TGS = bone/graft contact.

Table 2 Morphometric measurements of connectivity parameters under micro-CT (μCT) and under conventional histomorphometry (Histo)

	TbN (1/mm)		TbTh (μm)		TbSp (μm)	
	μCT	Histo	μCT	Histo	μCT	Histo
Sample 1	6.05	2.54	70	167.38	100	226.24
Sample 2	5.27	2.91	130	225.83	60	117.88
Sample 3	6.45	4.30	100	136.86	60	95.69
Mean	5.92	3.25	100	176.69	73.33	146.60
SD	0.60	0.92	30	45.21	23.09	69.85

TbN = trabecular number; TbTh = trabecular thickness; TbSp = trabecular separation.

Morphometric measurements

The morphometric parameters calculated by both the micro-CT and standard histomorphometry were: total volume (TV), total bone volume (TBV/TV), bone volume (BV/TV), trabecular thickness (TbTh), trabecular separation (TbSp), trabecular number (TbN), graft volume (GV/TV), total graft surface (TGS), and bone graft contact (BGC/TGS).

TBV/TV represents the total volume amount of the mineralized bone, plus that of the graft embedded in the bone matrix. BV/TV represents the amount of mineralized bone after subtraction of the graft volume (GV/TV). GV/TV represents the amount of graft particles still present in the specimens. Under standard histomorphometric evaluation the percentage of direct contact between particles of Biogran and bone trabeculae was calculated, and this value was expressed as a percentage of bone graft contact (BGC%) over the total surface of Biogran particles (GS).

The morphometric values obtained by micro-CT were compared with the values obtained by standard histomorphometric analysis. Micro-CT measurements were calculated from the mean of the values obtained from 400 slices (sections), while the histomorphometric measurements were as usual calculated from the mean of the values from three sections per sample.

The values obtained with the two different techniques were compared statistically using analysis of variance.

Results

The morphometric results from the standard histologic quantitative analysis and from the micro-CT are summarized in Tables 1 and 2.

The 3D reconstruction of the sequence on CT scan images from the micro-CT allowed the authors to find almost the same histologic section analyzed and also to correlate the 2D section with the 3D structures.

Micro-CT results

The mean TBV/TV measured 57.33%, the mean BV/TV measured 33%, and the mean GV/TV measured 24.33%. The mean structural values of connectivity were as follows: TbN = 5.92 (1/mm), TbTh = 100 μm, and TbSp = 73.33 μm.

Figure 1 is normalized with the total number of voxels (pixel^3) for each sample. The blue line, which refers to sample 1, shows a high peak on the left, indicating the presence of a lot of soft tissue and small amounts of bone and bioglass. Samples 2 and 3 showed an equal distribution of the voxel density between soft and hard tissues. Figure 2 is normalized with the number of bone voxels (voxels above 10,760) per sample. Sample 1 showed a higher percentage of bone than graft, whereas samples 2 and 3 had equal amounts of bone and graft.

Histologic and histomorphometric results

The mean TBV/TV measured 55.69%, the mean BV/TV measured 42.85% and the mean GV/TV measured 12.84%. The mean structural values of connectivity were: TbN = 3.25 (1/mm), TbTh = 176.69 μm, and TbSp = 146.6 μm.

Morphologic description of 3D and 2D micro-CT images

The visual assessment of the bony structure obtained with micro-CT produced several 2D slices and a 3D reconstruction of the specimens.

The 2D slices allowed the authors to distinguish most of the Biogran granules, which were often denser than the autogenous bone particles of the graft and of the bony trabeculae on radiographs. The 3D reconstructions gave a precise representation of the bone trabeculae and allowed visual exploration of the bone architecture in all parts of the biopsy.

The 3D reconstructions allowed the authors to obtain 3D images of bone and Biogran (Fig 3a), and by image subtraction, Biogran alone (Fig 3b), allowing the evaluation of the 3D distribution of all the grafted particles in the space. In some parts of the 2D and 3D sections, it was difficult to distinguish Biogran granules from the autogenous bone chips in the graft, because the radiodensity of the Biogran granules was very similar to that of the bone (Figs 3b and 3c).

Morphologic description of each sample analyzed

Sample 1

This sample was retrieved from the sinus after 5 months of healing. The bone graft inserted in the sinus was composed of 75% (by volume) Biogran and 25% autogenous bone. A PRP gel was added to the graft.

At micro-CT examination, three main radiodensities were observed. On one side was a very high density with a granular shape, which could presumably represent granules of Biogran (white), while on the other side was a dark gray structure with a morphology similar to that of thin bone trabeculae. A third structure with an intermediate radiodensity (between the Biogran and the bone trabeculae) was also visible. This structure had a different morphology from the Biogran particles and the bone trabeculae and could represent the autologous bone chips of the graft (see Fig 3c).

Histologic examination revealed that bone trabeculae appeared to be composed mainly of woven bone with many large rounded osteocyte lacunae (Fig 3d). Regions of osteoid formation and lamellar bone formation were found on bone surfaces. Resorption lacunae were also observed. Biogran particles were found embedded in new bone, showing the typical border staining and cracks (Fig 3e). Twenty-six percent of the graft particle surface was in contact with mineralized bone. The 3D micro-CT examination (Figs 3a and 3f) and the quantitative analysis of the bone structure revealed a TBV/TV of 43%, although this sample had healed for only 5 months. The 3D image of the biopsy showed a very dense bone structure (see Figs 3a and 3f). The visual analysis of the graft (see Fig 3b) obtained through the digital image subtraction gave an idea of the spatial distribution of the grafted particles, allowing the authors to recognize the shape of autogenous bone chips and of Biogran granules.

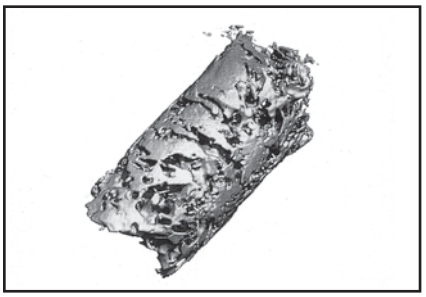

Fig 3a *Sample 1. Three-dimensional micro-CT reconstruction of a cylindric biopsy retrieved from a sinus grafted with Biogran after 5 months of healing. This sample shows a representation of the bone trabeculae (original magnification ×16).*

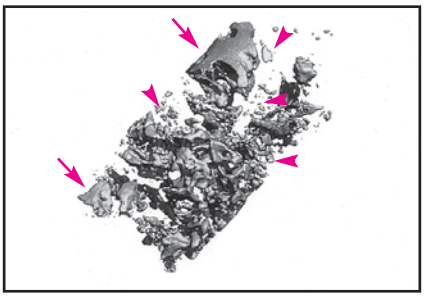

Fig 3b *Sample 1. Three-dimensional micro-CT image showing the spatial distribution of the graft in the biopsy. By applying the image subtraction technique, it was possible to subtract from the image all the parts under a certain threshold of radiodensity. In this way the grafting material could be distinguished from bone. In this image, two different shapes are evident: particles* (arrowheads), *probably Biogran granules, often broken into small parts, and particles* (arrows) *that closely resemble the autogenous bone chips of the graft (original magnification ×16).*

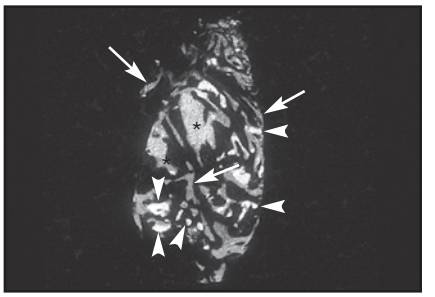

Fig 3c *Two-dimensional micro-CT analysis of sample 1. It is possible to observe three main radiographic densities. A very high density with a granular shape could presumably represent granules of Biogran* (arrowheads). *It is also possible to see dark gray structures with a morphology similar to that of thin bone trabeculae* (arrows). *A third structure is visible, with a radiodensity that is intermediate between the Biogran and the bone trabeculae, that could represent the autologous bone chips* (asterisks) *(original magnification ×16).*

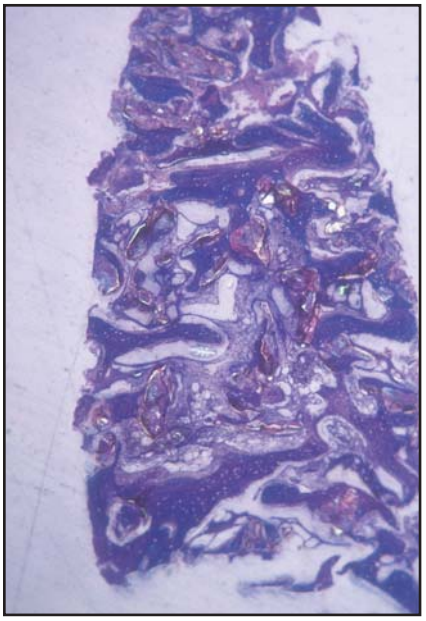

Fig 3d *Histologic overview of sample 1. Thin bone trabeculae are visible* (blue staining), *containing many large and rounded osteocytic lacunae. Small and crumbled pieces of Biogran are found between the bone and marrow tissues (toluidine blue; original magnification ×25).*

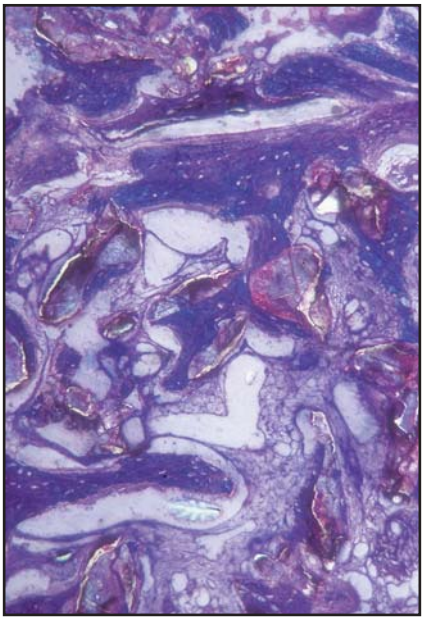

Fig 3e *Sample 1. Biogran particles were found embedded in new bone showing the typical border staining and cracks. Twenty-six percent of the graft particle surface is in contact with mineralized bone (toluidine blue; original magnification ×50).*

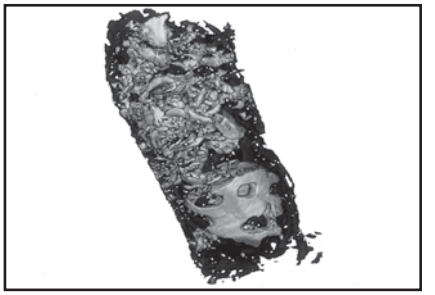

Fig 3f *Three-dimensional micro-CT overview of sample 1, showing the bone structure (original magnification ×16).*

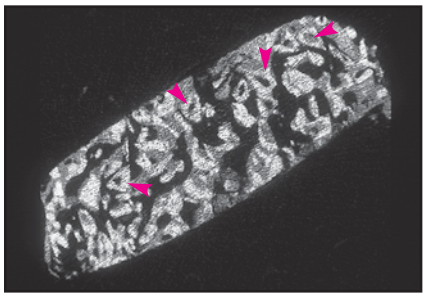

Fig 4a (top left) *Sample 2. A dense bone was found composed of thick trabeculae very well connected to each other* (dark gray). *Dense particles similar to granules of Biogran* (light gray), *mostly encased within mineralized bone, are evident* (arrowheads). *The particles are mostly broken into pieces or excavated into the center (2D micro-CT; original magnification ×16).*

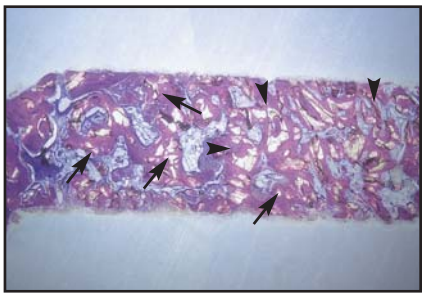

Fig 4b (top right) *Histologic overview of sample 2. The analysis revealed a dense trabecular bone composed of thick trabeculae that were very well connected to each other* (purple staining). *The particles of Biogran are visible as white spots with sharp edges into the bone trabeculae. These particles appear broken into pieces* (arrows) *and excavated in the center* (arrowheads). *The central excavations are often filled with bone (basic fuchsin and toluidine blue; original magnification ×25).*

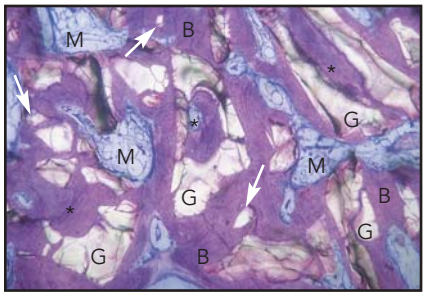

Fig 4c (bottom left) *Higher magnification of the sample shown in Fig 4b. Large amounts of Biogran particles were found encased in the bone matrix, mostly osseointegrated. The Biogran particles are disrupted in small pieces* (arrows) *or hugely excavated in the center and filled by bone* (asterisks) *(basic fuchsin and toluidine blue; original magnification ×200). B = bone; G = granules of Biogran; M = soft marrow tissue.*

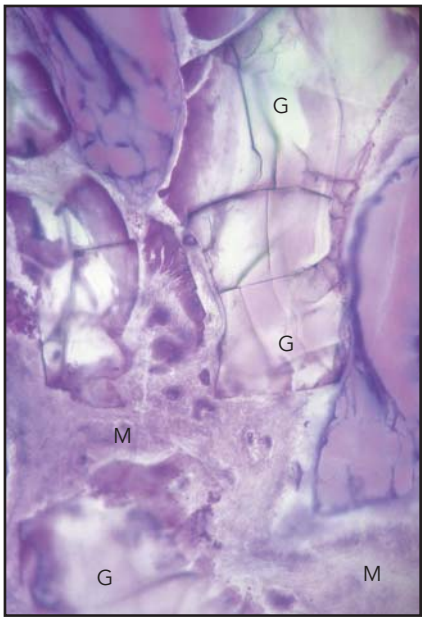

Fig 4d (bottom right) *In some places, the surfaces of the Biogran particles (G) exposed to the soft marrow tissue (M) are covered by macrophages digesting small parts of the graft (basic fuchsin and toluidine blue; original magnification ×400).*

Sample 2

This sample was retrieved from the sinus after 15 months of healing. The bone graft inserted in the sinus was composed of 90% (by volume) Biogran and 10% autogenous bone retrieved from intraoral donor sites.

The 2D micro-CT analysis showed dense bone composed of thick trabeculae that were very well connected to each other (Fig 4a). Radiopaque particles, similar to Biogran granules and mostly in contact with mineralized bone, were evident. Some of the particles seemed to be broken into pieces or excavated at the center. The central excavation was often filled by bone. The histologic examination confirmed these observations (Fig 4b); it also revealed that the bone matrix was mainly composed of lamellar bone, but in the central core of the trabeculae, some islands of woven bone were still present. The volume occupied by the Biogran particles, under histologic analysis, measured 16% of the total volume, while the mineralized bone occupied 50% of the total space of the biopsy. Sixty percent of the graft particle surfaces were in contact with mineralized bone. The bioglass particles had split into small pieces or were hugely excavated in the center and filled by bone (Fig 4c). The bone surfaces were mostly in a resting state, but signs of bone remodeling were also found. The surfaces of the Biogran particles exposed in the marrow tissues were covered by macrophages (Fig 4d).

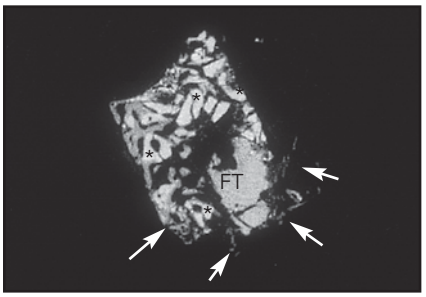

Fig 5a *Two-dimensional micro-CT analysis of sample 3. This sample revealed a trabecular bone structure, with numerous particles of Biogran and internal central excavations (asterisks) in the bone matrix and in soft tissue. In the lower part of the picture, a large, heavy, mineralized fragment of dense matrix is visible (FT), similar in shape and dimension to an autologous bone chip, also visible in the histologic section labeled A in Fig 5b. All around the heavy mineralized fragment, thin trabeculae of low radiodensity are present, possibly an expression of thin woven bone trabeculae (arrows) (original magnification ×20).*

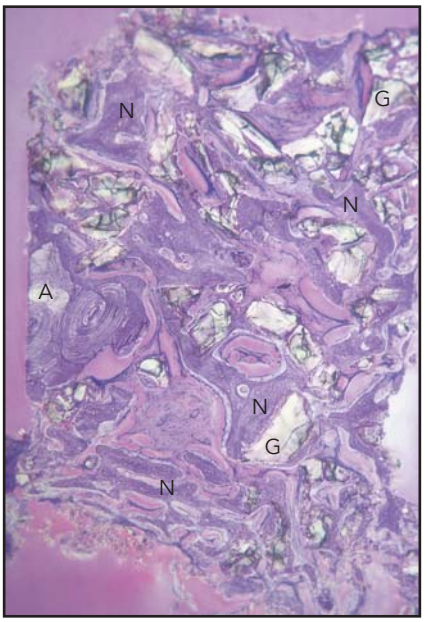

Fig 5b *Histologic overview of sample 3. Dense trabecular bone, mainly woven bone, was found in this sample. Many Biogran particles (G) are visible embedded in the new bone (N), and a large autologous bone chip was also found (A; see FT in Fig 5a) (basic fuchsin and toluidine blue; original magnification ×50).*

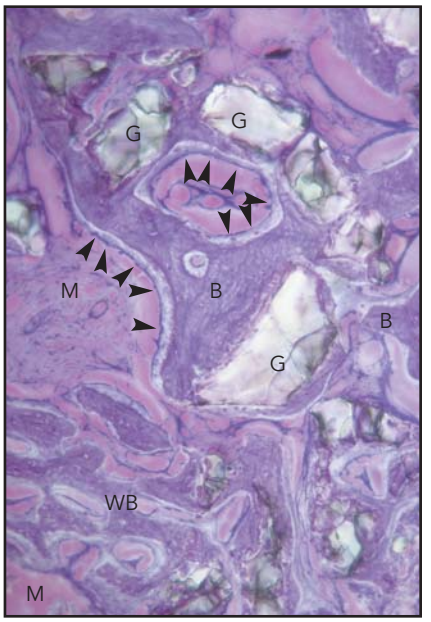

Fig 5c *Higher magnification of the sample shown in Fig 5b. The bone surfaces are covered almost everywhere by layers of osteoid (arrowheads). A fine woven bone network (WB) is present (basic fuchsin and toluidine blue; original magnification ×100). B = bone; G = granules of Biogran; M = soft marrow tissue.*

Examination of the 3D micro-CT reconstruction revealed very dense bone, with thick trabeculae that were very well connected to each other. The subtraction analysis showed many small radiographically dense particles—probably Biogran particles—that were broken into small pieces and dense particles similar to the autogenous bone chips of the graft.

Sample 3

This sample was retrieved from a grafted sinus after 6 months of healing. The sinus was grafted with a mixture of Biogran (75% by volume) and 25% autogenous bone, retrieved from intraoral donor sites and minced into particles. A PRP gel was added to the graft.

At the 2D micro-CT examination (Fig 5a), this sample revealed a dense trabecular bone with particles of Biogran in the bone matrix and in soft tissue. Some particles of Biogran revealed an internal central excavation with bone inside. Other particles appeared to be crumbled into pieces, mostly surrounded by bone. In some parts of the biopsy, very thin trabeculae of a low radiodensity were present, possibly an expression of thin woven bone trabeculae. The histologic analysis (Figs 5b and 5c) showed that most of the new bone was woven. Many particles and some large autologous bone chips were visible in the histologic sections (see Fig 5b), whose extended shape resembled the images on the micro-CT reconstruction. The bone surfaces were covered by layers of osteoid almost everywhere (see Fig 5c). Particles of Biogran were found embedded in the bone matrix and in contact with the soft tissues. Forty-five percent of the Biogran surfaces were in contact with mineralized bone. Also, particles of autologous bone chips were found (see Fig 5b) surrounded by new woven bone.

Examination of the 3D reconstruction revealed dense bone. The

subtraction analysis revealed radiopaque particles that closely resembled bone chips of the graft.

Statistical comparison of the results

Comparing the results obtained by conventional histomorphometry and micro-CT, we observed that:

- The values for TBV/TV obtained by both methods were very similar in all the samples, without statistically significant differences.
- The values of BV/TV obtained by histomorphometry were always higher (by about 30%) than those obtained by micro-CT, but without statistically significant differences.
- The values of GV/TV obtained by histomorphometry were always lower than those obtained by the micro-CT, but without statistically significant differences.
- The values of TbN obtained by histomorphometry were lower than those obtained by micro-CT and were statistically significantly different.
- The values of TbTh and TbSp obtained by micro-CT were lower than those obtained with histomorphometry, but without statistically significant differences.

Discussion

The density of regenerated bone is often very low after a few months of healing and depends on the time of healing[32] as well as on the density of the preexisting bone around the defect.[33] However, the load applied under function to implants placed in the posterior maxilla is very high because posterior teeth are in close proximity to the temporomandibular joint. It is therefore important to clearly analyze the 3D architecture of the regenerated bone after sinus grafting and its relationship with its mechanical competence to better clarify the healing time of the graft and the implants and to determine what loading conditions to apply.

In 1989 Feldkamp et al[26] introduced an x-ray micro-CT system to create 3D images. More recent developments[34] allowed the creation of higher-resolution 3D images and quantitative measurements of the trabecular bone structure.[27]

Micro-CT was validated as a method for the 3D assessment and analysis of cancellous bone by Muller et al in 1998, who compared the morphometric results of conventional histomorphometry to results of micro-CT.[35] These authors demonstrated the strength of 3D representation of trabecular bone architecture in comparison with conventional 2D histology, showing excellent correlation of the indices assessed. Recent studies have proposed the application of micro-CT for dental implant research.[36,37]

The mechanical properties of bone largely depend on the 3D structure,[24,38,39] which is measured by the bone volume and the connectivity indexes. The ultimate goal of any bone measurement in patients is to estimate bone strength.[31,38] Because most regenerative procedures are performed to obtain strong tissue to support implant placement, it is important to precisely quantify bone microarchitecture with a 3D technique, such as micro-CT 3D analysis.

To the authors' knowledge, micro-CT techniques have not been used to perform a 3D quantitative evaluation of bone biopsies containing hard biomaterials from the maxillary sinus. To validate micro-CT measurements, it is very important to compare the data obtained by standard histomorphometry to the data obtained using micro-CT in the same biopsy sample. This is possible because micro-CT is a nondestructive technique that allows subsequent histologic analysis.

All the samples analyzed in the present study showed that the 2D histologic analysis gave almost the same results, without statistically significant differences in TBV/TV, as the 3D micro-CT scanning. Other evaluated variables did not show statistically significant differences, even when the mean values were quite different. These differences were particularly evident in the micro-CT measurements of BV/TV, which were always lower, and the micro-CT measurements of GV/TV, which were always elevated versus the histomorphometric measurements. This fact could be explained by the physical characteristics of the radiopaque graft material that was inserted in the sinuses, which was a mixture of autogenous bone and Biogran, which have similar radiodensity. For this reason, the histogram analysis of the gray levels (see Fig 2) shows a superimposition of a part of the peaks, which certainly caused a modification of the quantitative micro-CT results of BV/TV and GV/TV. This was particularly evident at the 3D examination of the GV/TV after subtraction analysis (see Fig 3c), where we expected to find only bioglass particles but also found radiopaque particles that closely resembled the bone chips that were added to the graft. Moreover, under histologic analysis we could not distinguish between newly formed bone and grafted autologous bone because of the difficulty in clearly identifying the latter. After some months of healing, Biogran particles seemed to be broken into small pieces. Very small bioglass fragments were much more difficult to detect with resolution of the micro-CT and also with visual 3D analysis. The lack of statistically significant differences could also be a result of the small number of samples and large variations between samples in the same group.

The histologic examination showed the same differences between samples, but the connectivity values obtained from the micro-CT were quite different from the corresponding histologic values. This may be a result of the 2D limitation of the histologic analysis for parameters that reflect a structural

spatial organization, as do the connectivity indexes.

Sample 1 had low percentages of new bone and Biogran. In contrast, samples 2 and 3 were quite similar and demonstrated a very dense BV/TV and a higher percentage of Biogran overall. However, sample 1 had healed for only 5 months. This could explain the differences found between sample 1 and sample 2, which had healed for 15 months, and the smaller differences between sample 1 and sample 3, which had healed for only 6 months. However, the differences between samples 1 and 3 were particularly evident when examining the total bone volume (TBV/TV) obtained, while they seemed to be less evident in examining vital bone volume (BV/TV). Another observation was the similar total bone volume (TBV/TV) obtained in samples 2 and 3. Sample 2 had healed for 15 months but did not include PRP. Sample 3 had healed for 6 months but did include PRP. This could indicate that PRP might favor or accelerate new bone formation. But PRP was also included in the sample 1 graft, and the percentage of total bone volume was still lower after 5 months. However, a percentage of total bone volume around 40%, although it was lower than in the other samples, is sufficient for predictable implant placement and can be considered a satisfying percentage of new bone formed if it is taken into account that the graft had healed for only 5 months. Moreover, the percentage of vital bone volume (BV/TV) obtained was 37.53% after 5 months and 41.32% after 6 months. These are notable results that might be explained by the positive effects of PRP or Biogran on bone regeneration or by the combination of both.

With the limitation of the small number of samples analyzed, the results of the present study also showed that PRP added to a mixture of autogenous bone and Biogran could improve the new bone formation, with a reduction in the time needed for the graft healing and a high quantity of bone formed after only 5 to 6 months.

Moreover, micro-CT was shown to be a fast, nondestructive procedure that allowed measurement of trabecular and compact bone and of the radiopaque grafting materials in unprocessed biopsies as well as an automatic determination of 3D structural morphometric indices. The encouraging data collected in this series of three case reports encourage us to continue this study. In the future, micro-CT might help us to investigate the relative importance of bone architecture as a better index of bone strength, especially when used in combination with histologic study.

References

1. Brånemark P-I, Zarb GA, Albrektsson T (eds). Tissue-Integrated Prostheses. Chicago: Quintessence, 1985:241–282.
2. Misch CE, Judy WMK. Classification of the partially edentulous arches of implant dentistry. Int J Oral Implantol 1987;4:49–58.
3. Albrektsson T, Brånemark P-I, Hansson HA, Lindstrom J. Osseointegrated titanium implants. Requirements for ensuring a long-lasting, direct bone-to-implant anchorage in man. Acta Orthop Scand 1981;52(2):155–170.
4. Jensen OT, Schulman LB, Block MS, Iacono VJ. Report of the Sinus Consensus Conference of 1996. Int J Oral Maxillofac Implants 1998;13(suppl):11–32.
5. Lazzara RJ. The sinus elevation procedure in endosseous implant therapy. Curr Opin Periodontol 1996;3:178–183.
6. Tatum OH Jr. Maxillary and sinus implant reconstructions. Dent Clin North Am 1986;30:207–229.
7. Jensen OT. Allogenic bone or hydroxylapatite for the sinus lift procedure? J Oral Maxillofac Surg 1990;48:771–776.
8. Blomquist EJ, Alberius P, Isaksson S. Sinus inlay bone augmentation: Comparison of implant positioning after one or two stage procedures. J Oral Maxillofac Surg 1997;55:804–810.
9. Boyne PJ, James RA. Grafting of the maxillary sinus floor with autogenous marrow and bone. Oral Surg 1980;38:613–616.
10. Cawood JI, Stoeling PJ, Bonus JJ. Reconstruction of the severely resorbed (class VI) maxilla: A two step procedure. J Oral Maxillofac Surg 1994;23:219–225.
11. Kent JN, Block MS. Simultaneous maxillary sinus floor bone grafting and placement of hydroxylapatite-coated implants. J Oral Maxillofac Surg 1989;47:238–242.
12. Wetzel AC, Stich H, Caffesse RG. Bone apposition onto oral implants in the sinus area filled with different grafting materials: A histologic study in beagle dogs. Clin Oral Implants Res 1995;6:155–163.
13. Wheeler SL, Holmes RE, Calhoun CJ. Six-year clinical and histologic study of sinus graft. Int J Oral Maxillofac Implants 1996;11:26–34.
14. Szabo G, Suba Z, Divinyi T, Haris A. HTR polymer and sinus elevation: A human histologic evaluation. J Long Term Eff Med Implants 1992;2:81–92.
15. Wallace SS, Froum SJ, Tarnow DP. Histologic evaluation of sinus elevation procedure: A clinical report. Int J Periodontics Restorative Dent 1996;16:47–51.
16. Garetto LP, Chen J, Parr JA, Roberts WE. Remodeling dynamics of bone supporting rigidly fixed titanium implants: A histomorphometric comparison in four species including humans. Implant Dent 1995;4:235–243.
17. Wennerberg A, Albrektsson T, Andersson B, Krol JJ. A histomorphometric and removal torque study of screw-shaped titanium implants with three different surface topographies. Clin Oral Implants Res 1995;6:24–30.
18. Frost HM. A determinant of bone architecture. The minimum effective strain. Clin Orthop 1983;275:286–292.
19. Frost HM. The skeletal intermediary organization. Metabol Bone Dis Relat Res 1983;4:281–290.
20. Frost HM. The regional acceleratory phenomenon: A review. Henry Ford Hosp Med J 1983;31:3–9.
21. Parfitt AM, Mathews CH, Villanueva AR, Kleerekoper M, Frame B, Rao DS. Relationships between surface, volume, and thickness of iliac trabecular bone in aging and in osteoporosis. Implications for the microanatomic and cellular mechanisms of bone loss. J Clin Investig 1983;72:1396–1409.
22. Roberts WE, Garetto LP, DeCastro RA. Remodeling of devitalized bone threatens periosteal margin integrity of endosseous titanium implants with threaded or smooth surfaces: Indications for provisional loading and axially directed occlusion. J Indiana Dent Assoc 1989;68: 19–24.

23. Trisi P, Rebaudi A. Progressive bone adaptation of titanium implants during and after orthodontic load in humans. Int J Periodontics Restorative Dent 2002;22: 31–43.

24. Mosekilde L. Consequences of the remodelling process for vertebral trabecular bone structure: A scanning electron microscopy study (uncoupling of unloaded structures). Bone Miner 1990;10:13–35.

25. Odgaard A, Andersen K, Melsen F, Gundersen HJ. A direct method for fast three-dimensional serial reconstruction. J Microsc 1990;159(Pt 3):335–342.

26. Feldkamp LA, Goldstein SA, Parfitt AM, Jesion G, Kleerekoper M. The direct examination of three-dimensional bone architecture in vitro by computed tomography. J Bone Miner Res 1989;4:3–11.

27. Ruegsegger P, Koller B, Muller R. A microtomographic system for the nondestructive evaluation of bone architecture. Calcif Tissue Int 1996;58:24–29.

28. Donath K, Breuner G. A method for the study of undecalcified bones and teeth with attached soft tissues. The Sage-Schliff (sawing and grinding) technique. J Oral Pathol 1982;11:318–326.

29. Chappard D, Legrand E, Pascaretti C, Basle MF, Audran M. Comparison of eight histomorphometric methods for measuring trabecular bone architecture by image analysis on histological sections. Microsc Res Tech 1999;45:303–312.

30. Recker RR. Bone Histomorphometry: Technique and Interpretation. Boca Raton, FL: CRC Press, 1983.

31. Rebaudi A, Trisi P. Micro-computed tomographic analysis of the peri-implant bone. J Periodontics Restorative Dent 2004;24:316–325.

32. Trisi P, Rao W. The bone growing chamber: A new model to investigate spontaneous and guided bone regeneration of artificial defects in the human jawbone. Int J Periodontics Restorative Dent 1998;18:151–159.

33. Trisi P, Rao W, Rebaudi A, Fiore P. Histologic effect of pure-phase beta-tricalcium phosphate on bone regeneration in human artificial jaw bone defects. Int J Periodontics Restorative Dent 2002;23: 69–77.

34. Hildebrand T, Ruegsegger P. Quantification of bone microarchitecture with the Structure Model Index. Comput Methods Biomech Biomed Engin 1997;1:15–23.

35. Muller R, Van Campenhout H, Van Damme B, et al. Morphometric analysis of human bone biopsies: A quantitative structural comparison of histological sections and micro-computed tomography. Bone 1998;23:59–66.

36. Rebaudi A, Trisi P. MicroCT scan: A new technique to investigate periimplant bone [abstract 47]. Clin Oral Implants Res 2000;11:396.

37. Sennerby L, Wennerberg A, Pasop F. A new microtomographic technique for non-invasive evaluation of the bone structure around implants. Clin Oral Implants Res 2001 Feb;12(1):91–94.

38. Dalstra M, Huiskes R, Odgaard A, van Erning L. Mechanical and textural properties of pelvic trabecular bone. J Biomech 1993;26:523–535.

39. Roberts WE, Simmons KE, Garetto LP, DeCastro RA. Bone physiology and metabolism in dental implantology: Risk factors for osteoporosis and other metabolic bone diseases. Implant Dent 1992;1:11–21.